The synthesis of Fe_3O_4 spherical particles with defined size in a liquid medium

A. E. Dosovitskii,[a] E. V. Grishechkina,[a] A. L. Mikhlin,[a] V. M. Retivov,[a] A. V. Sobolev,[b] I. A. Presnyakov,[b] and Yu. O. Lekina[b]*

[a] *Institute of Chemical Reagents and High Purity Chemical Substances, 3 ul. Bogorodskiy val, 107076 Moscow, Russian Federation. E-mail: el.v.gulyaeva@gmail.com*
[b] *M. V. Lomonosov Moscow State University, Chemistry Department, Build. 3, 1 Leninskie Gory, 119991 Moscow, Russian Federation*

A method for the preparation of nano- and submicron spherical particles of magnetite which form agglomerates was described. At varying the reaction conditions, the particles of ~50—200 nm were obtained and characterized by scanning electron microscopy, IR-spectroscopy, X-ray analysis, thermogravimetric analysis and differential scanning calorimetry. The scheme (zero approach) of the magnetite formation in the studied system was proposed. The investigation of magnetic properties proved that the obtained particles related to the hard magnetic materials. Curie temperature for the particles with different sizes was detected.

Key words: nanoparticles, submicron particles, magnetite, Fe_3O_4, liquid phase sinthesys.

Synthesis of nano- and submicroparticles with a narrow size distribution opens the possibilities of the detailed investigation of their properties, size effects study as well as fabrication of composite materials with specified characteristics, which include these particles. Particles with a narrow size distribution are of a great interest from both fundamental and practical points of view. Among the magnetic materials, much attention of scientists and technologists has been focused on magnetite particles (Fe_3O_4). Despite the production of nano- and submicron particles have been developing since the end of XX century, an interest to these materials is still growing. So according to the data of Sciencedirect website, a number of annual publications on magnetite nanoparticle synthesis increased from 35 to 1308 during the time period from 1997 to 2015 (data from august, 2015). Fe_3O_4 nanoparticles are considered to be promising for such applications as contrast agents for the magnetic-resonance imaging, magnetic separation, hyperthermia,[1—5] at production of the two- or three-dimensional ordered structures for photonics,[6,7] *etc*.

Synthesis in liquid media (liquid-phase synthesis) is the most perspective method for production of magnetite nanoparticles as it enables to control effectively the stages of nucleation and particle growth by varying reaction conditions.[8,9] Nowadays, spherical nano- and submicron particles of magnetite with a narrow size distribution are generally produces by solvothermal reduction of iron(+3) salts in polyols used as a dispersion media. This technique for the nanoparticle formation is referred to as polyol synthesis in the literature. The mentioned approach has been known for about 20 years.[9] The choice of polyols resulted from their properties. They are polar dispersion media and mild reducing agents, additionally, characterized with high boiling points. The described procedures of formation of nano- and submicron particles by this method[10—13] involve utilization of an autoclave or a base as a precipitating agent, as well as the reaction was performed at temperatures above 180 °C.

In this work, we suggested a modified approach to the synthesis of nano- and submicrom Fe_3O_4 particles of specified size by high temperature reduction of iron(+3) salts at temperatures below 180 °C without need in utilization of an autoclave and a base. The obtained particles represent spherical agglomerates with the smaller size particles. Magnetite particles with the mean size of 50—200 nm were produced by varying the reaction conditions.

Experimental

Iron(+3) chloride hexahydrate $FeCl_3 \cdot 6H_2O$ (analytical grade), sodium acetate trihydrate $C_2H_3NaO_2 \cdot 3H_2O$ (analytical grade), ethylene glycol $C_2H_6O_2$ (analytical grade), polyethylene glycol-400 (PEG-400) (analytical grade) were used without additional purification.

The idea of the method is a partial reduction of iron(+3) to iron(+2) at the enhanced temperature and the reaction between iron(+3) and iron(+2) compounds which results in magnetite formation. The reaction time was varied from 0.5 to 8.0 h. The mole ratio $C_2H_3O_2Na : Fe^{3+}$ was varied from 3 : 1 to 15 : 1. The initial concentration of iron(+2) cations was 0.05 mol L^{-1}, temperature 175 °C. PEG-400 was used as a stabilizer, which concentration was ranged from 0 to 10 mmol L^{-1}. Ethylene glycol was applied as a solvent.

Published in Russian in *Izvestiya Akademii Nauk. Seriya Khimicheskaya,* No. 3, pp. 0704—0713, March, 2016.

The size and morphology of the synthesised particles was defined by scanning electron microscopy on Hitachi SU 1510 and Jeol JSM 7100 F microscopes. The average size and the size distribution, as well as ζ-potential of nano- and submicron particles were defined by dynamic light scattering and electrophoresis using a Zetasizer Nano (Malvern) analyzer. To determine an average size and size distribution of micron-sized particles, Mastersizer Nano (Malvern) device was applied.

The X-ray diffraction (XRD) analysis was performed on Emma (GBC Scientific), by using Cu-Kα irradiation (λ = 1.542 Å). The interval of registrated angles was 10—90° with a step of 0.02°.

IR spectra were recorded on a Fourier transform infrared spectrometer (VERTEX 70/70v) in the range of 7500—400 cm^{-1} with a resolution of 4 cm^{-1} at 22 °C. A spectrum of analytical grade KBr was applied as a background spectrum.

Thermogravimetry (TGA) and differential scanning calorimetry (DSC) measurements were carried out on SDT Q600 (TA Instruments) equipment in the temperature range from 30 to 1000 °C at a heating rate of 5 °C min^{-1} in both inert and air atmosphere. Thermal analysis was performed using a powder which was not heated beforehand.

The product yield was determined from the residual content of iron(+3) in the initial solution after the magnetite particles were synthesized. The procedure followed the adapted protocol in RF state standart GOST 10398-76 "The complex method for determination of the content of the main component".

Magnetic properties were measured on a vibrating sample magnetometer (Lakeshore, model 7407) in a magnetic field up to 16 kOe.

The hysteresis loops were registered at room temperature (300 K). Samples were places in polyethylene bags sized 5×5 mm, weighted, compressed (to minimize particle movement inside a bag) and sealed. The bags were immobilized on quarts holders by means of Teflon tape.

Mössbauer spectra was recorded on a MS_1104Em spectrometer at 300 K. Mössbauer experiments were carried out in transition geometry in a constant acceleration mode with a triangle form of time dependency of Doppler rate of absorber movement with respect to a source. The spectrometer divided the velocity scale into 1024 channels. Hence, before processing, the recorded spectra were transformed by summation of four adjacent channels and represented into 256 channels. Thus, after the preliminary processing, spectra contain 256 points. Such transformation results in an improved quality of a spectrum.

^{57}Co in a rhodium matrix was used as a source of gamma-radiation. Calibration was performed using α-Fe metal patterns.

Results and Discussion

Practical application of magnetite spherical particles contemplates a proven and reproducible technique of synthesis. Hence, in order to define the optimal reaction parameters, the influence of conditions on size and morphology of the particles were studied.

Correlation between magnetite particle size and reaction time. It is known[14], that formation of spherical particles of magnetite in an autoclave proceeds for a long time. Since our approach for the magnetite spherical particle production does not involve the autoclave utilization, the reaction time may differ from that mentioned in scientific literature.

In order to define the optimal reaction time for Fe_3O_4 particle generation, several probes were collected from the reaction mixture at different time and the size and morphology of the formed particles were determined. The initial concentration of iron(+3) salt was 0.05 mol L^{-1}, mole ratio was $C_2H_3O_2Na$: Fe^{3+} = 9 : 1, the synthesis proceeded for 8 h.

According to the data of scanning electron microscopy, magnetite particles with a size of less than 50 nm, which were disposed on the surface of micron-sized particles, were formed in 0.5 h after the reaction started (Fig. 1, *a*). Increasing reaction time up to 1.0 h resulted in formation of spherical particles with a diameter less than 150 nm (Fig. 1, *b*). However, along with the separated spherical particles, a noticeable amount of agglomerates were found in the reaction mixture. That is why the histogram of the particle-size distribution, which was obtained from the data of the dynamic light scattering analysis, shows the maximum corresponding to the submicroparticles with the mean size of *ca.* 700 nm (Fig. 1, *b*, insert). Particles, which were formed in 0.5 and 1.0 h after the reaction started, have a wide size distribution and were present in the system with different fractions (as follows from the data obtained by dynamic light scattering and scanning electron microscopy). Thus in 0.5 h particles with an average diameter of 820 nm, 5.6 and 3.3 μm were formed; in 1.0 h the average particle size was 700 nm, 1.8 and 6.6 μm. Fe_3O_4 particles synthesized within 2.0 h seems to represent nano- and submicron spheres (Fig. 1, *c*). The mean particle size was 173 nm, as it followed from the histogram of particle-size distribution. With increasing reaction time for 1.0 h the size distribution was nearly constant. In 4.0 h after the synthesis started, the particle-size distribution decreased for ~5 nm. The further reaction time increase almost did not influence the particle size, their dispersion and morphology.

High resolution scanning electron microscopy study showed that the obtained spherical particles represented agglomerates of particles of 5—15 nm (Fig. 1, *g*). Probably during the synthesis particles of the mentioned size were formed followed by aggregation and production of the spherical structures with diameter of 173±20 nm.

Thus, based on the obtained results, we can conclude that 4 h is sufficient time for generation of spherical particles with the narrow size distribution. In order to define the time required for the magnetite generation as well as to clarify the scheme of its formation, X-ray diffraction analysis of the particles sampled at different reaction time was carried out.

The supposed scheme of the synthesis. In order to define the time required for the magnetite generation as well as to clarify the scheme of its formation, X-ray diffraction analysis of the particles sampled at different reaction time.

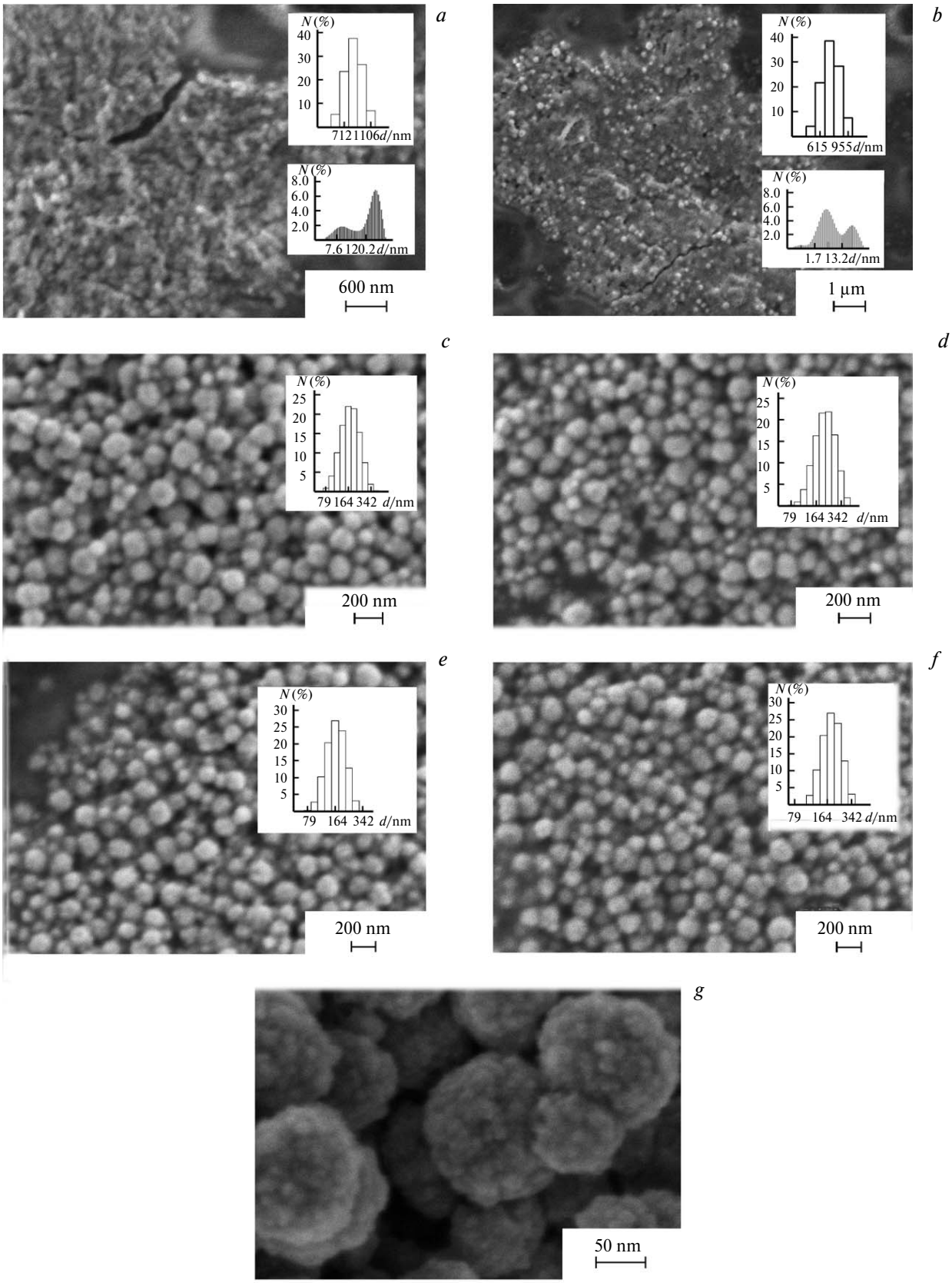

Fig. 1. SEM images of magnetite particles, obtained at different reaction time: 0.5 (*a*), 1.0 (*b*), 2.0 (*c*), 3.0 (*d*), 6.0 (*e*) and 8.0 h (*f*); surface morphology of magnetite particles (*g*). In insertion, particle-size distribution; *N* is a volume fraction, *d* is a particle size.

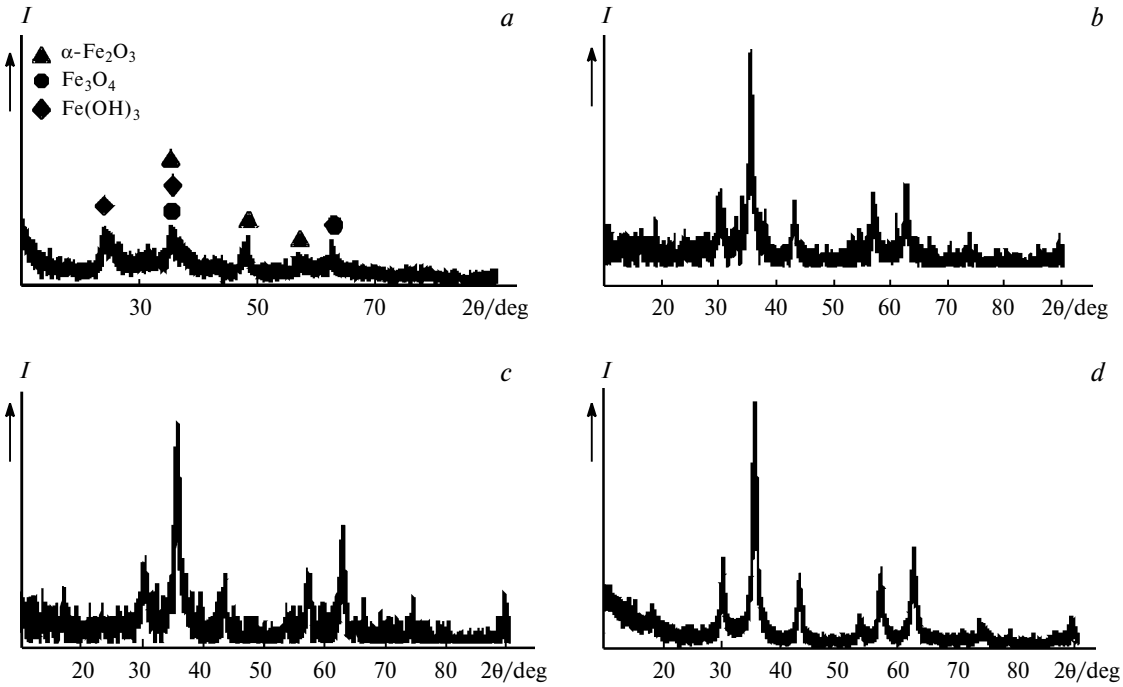

Fig. 2. XRD patterns of the samples registered at different reaction time: 0.5 (*a*), 1.0 (*b*), 2.0 (*c*), and 3.0 h (*d*).

The particles obtained at the initial concentration of iron(+2) salt of 0.05 mol L^{-1} and the mole ratio $C_2H_3O_2Na : Fe^{3+} = 9 : 1$ were investigated. The synthesis proceeded for 8 h.

In 30 min after the reaction started, an amorphous phase is generally present in the system (Fig. 2, *a*) and the other phases, which are likely to be iron(+3) hydroxide, hematite (α-Fe_2O_3) and magnetite just start forming. Magnetite formation is not definite as it is isostructural to maghemite (γ-Fe_2O_3).[15—17] Maghemite forms a continuous series of solid solutions with magnetite that makes their unequivocal identification via X-ray diffraction difficult, especially in the nanoscale state. The given peaks of low intensity can represent a superposition of several responses.

The XRD results showed that in 1 h after the reaction started, magnetite with a spinel structure, attributing to $Fd\bar{3}m$ space group, is formed (Fig. 2, *b*). The XRD profiles of the studied samples were typical of the single-phase state and no signs of asymmetry of the (511) line corresponding to the bi-phasic (magnetite—maghemite) state were found.[16] At the extended reaction time magnetite is formed. The diffraction lines corresponding to magnetite particles are remarkably broaden. That indicates on the small size of the given particles. Low intensity of the background line (6—8% of the most intensive peak) and an amourphous halo presence give evidence to the amorphous phase presence in the sample.

The formation mechanism of magnetite spherical particles in a similar system but at 200 °C using an autoclave has been reported.[10]

Scheme 1

$$2\,Fe^{3+} + Ac^- + 5\,H_2O \longrightarrow Fe_2O(Ac)(OH)_3 \cdot H_2O + 5\,H^+$$

$$Fe_2O(Ac)(OH)_3 \cdot H_2O \longrightarrow 2\,FeOOH + HAc + H_2O$$

$$4\,Fe_2O(Ac)(OH)_3 \cdot H_2O + 3\,C_2H_6O_2 \longrightarrow 8\,Fe + 3\,C_2H_2O_4 + 4\,HAc + 14\,H_2O$$

$$4\,Fe_2O(Ac)(OH)_3 \cdot H_2O + C_2H_6O_2 \longrightarrow 8\,Fe(OH)_2 + C_2H_2O_4 + 4\,HAc + 2\,H_2O$$

$$2\,FeOOH \longrightarrow Fe_2O_3 + H_2O$$

$$4\,Fe_2O_3 + Fe \longrightarrow 3\,Fe_3O_4$$

$$2\,FeOOH + Fe(OH)_2 \longrightarrow Fe_3O_4 + 2\,H_2O$$

The suggested mechanism (see Scheme 1) gives rise to doubt as oxalic acid formed during the synthesis is a complexing agent and is able to dissolve iron oxides partly.

Based on XRD data (see Fig. 2), the mechanism outlined above[10] was specified. We suggested a scheme describing the processes which were able to proceed in the considered system during the magnetite particle synthesis.

Sodium acetate reacting with Fe^{3+} gives characteristic tea-red color due to the formation of complex ions of $[Fe_3(CH_3COO)_6(OH)_2]^+$ iron(+3) hexacetate. At heating sodium acetate with Fe^{3+} cations, the main $Fe(OH)_2CH_3COO$ iron acatate is formed at the first stage:

$$Fe^{3+} + 3\ CH_3COO^- + 2\ H_2O \longrightarrow$$

$$\longrightarrow Fe(OH)_2CH_3COO + 2\ CH_3COOH.$$

Then the following reaction proceed:

$$Fe(OH)_2CH_3COO \longrightarrow \alpha\text{-}FeOOH + CH_3COOH.$$

Evaporation of acetic acid from the reaction mixture during the synthesis, as its boiling point (118 °C) is significantly lower than that of the reaction mixture (175 °C), leads to the change in pH of the system. At temperatures above 100 °C and pH close to a neutral solution, small crystallites of α-Fe_2O_3 are formed:

$$2\ Fe(OH)_3 \longrightarrow \alpha\text{-}Fe_2O_3 + 3\ H_2O.$$

Further increase in pH results in an increase in the crystallite sizes and the spherical α-Fe_2O_3 particles generation.[18] The experimental data confirm the change in pH during the synthesis supports. Thus for the given system, pH of the initial reaction mixture was 6.11 while after the reaction pH of the solution was *ca*. 8.

After that, the next reaction takes place:

$$\alpha\text{-}FeOOH + H_2O \longrightarrow Fe(OH)_3.$$

For the magnetite generation the presence of Fe^{2+} cations is needed. However, the registrated XRD data do not confirm the presence of iron(+2) compounds in the studied samples. We can suppose that the formed Fe^{2+} cations immediately react forming magnetite. Ethylene glycol operates as a reducing agent. The product yield of ~100% was defined by the residual content of iron(+3) in the solution.

Based on the obtained results, we can conclude that magnetite phase generates in 1 h after the reaction started.

The following investigations, presented in this work, were performed for the particles synthesized within 4 h.

Influence of the stabilizer content. It is known that with diminishing the particle size, the surface energy increases and aggregation of particles occurs as a result. Utilization of a stabilizer enables to decrease the surface energy and prevent particle agglomeration. In order to determine the optimal concentration of PEG-400, applied as a stabilizer, the correlation between its initial content and the mean particle size was obtained. Magnetite particles obtained without PEG-400 were used as a model system for comparison.

The starting concentration of iron(+3) salts was 0.05 mol L^{-1}, the mole ratio $C_2H_3O_2Na$: Fe^{3+} was equal to 9 : 1, PEG-400 concentration was varied from 0 to 10 mmol L^{-1}.

The results of the analyses of particles by dynamic light scattering and scanning electron microscopy are present in Table 1. Based on the obtained data we can conclude that at concentration of PEG-400 less than 5.0 mmol L^{-1}, particles with sizes up to ~3 μm were generated in the system, while at concentration more than 5.0 mmol L^{-1} , the average particle size was ~170 nm.

When adsorbed on the particle surface, the molecules of stabilizer prevent the following aggregation. For the practical application of the as-obtained spherical particles of magnetite, the residue needs to be washed from the excess of the stabilizer and products which are soluble in ethylene glycol. For the qualitative measurements of stabilizer molecules on the surface of particles after the washing, the obtained particles were characterized by IR spectroscopy.

The presence or absence of any main lines in the IR spectrum of the studied substance gives evidence to the presence or absence of functional groups characterized by the given absorption. The ensemble of all the absorption bands of the investigated material unambiguously identifies it. For the interpretation of the obtained data, model spectra of PEG and Fe_3O_4, as well as ethylene glycol (not presented) were applied.

In the IR spectrum of the stabilizer used in the present study, the characteristic bands corresponding to the func-

Table 1. The influence of synthesis conditions on size of magnetite particles (Fe^{3+} concentration is 0.05 mol L^{-1})

Concentration of PEG-400/mmol L^{-1}	$C_2H_3O_2Na$: Fe^{3+} (mol.)	Particle size/nm	Morphology
0	9 : 1	2660±520	Agglomerates of spherical particles
2.5	9 : 1	1910±350	Agglomerates of spherical particles
5.0	3 : 1	90±40	Spheres
	5 : 1	130±40	Spheres
	7 : 1	150±40	Spheres
	9 : 1	173±20	Spheres
	12 : 1	190±30 and ~800	Spheres and agglomerates of spherical particles
	15 : 1	200±50 and ~3000	Spheres and agglomerates of spherical particles
10.0	9 : 1	170±20	Spheres

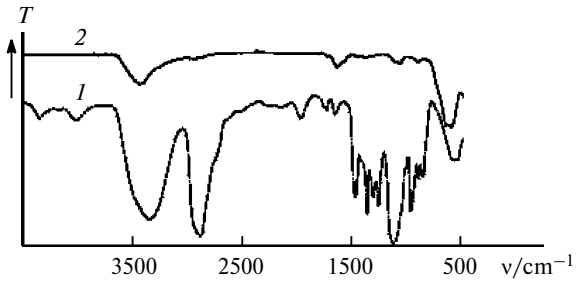

Fig. 3. IR spectra of PEG-400 (*1*) and the obtained magnetite particles (*2*); *T* is transmittance.

tional groups of PEG-400 (Fig. 3) were observed. Bands at 1110, 1249 and 1297 cm^{-1} correspond to the stretching vibrations of —C—O—C— group, bands at 1351 and 1455 cm^{-1} correspond to the deformation vibrations of $\delta(CH_2)$. The peak at 2871 cm^{-1} is likely to be related to the overlapped bands characterizing the asymmetric and symmetric stretchings of CH_2-groups. In the long-wavelength region of the spectrum, a broaden absorption band at 3349 cm^{-1} was registered which corresponds to the stretching vibrations of the bonded OH-groups. The obtained data indirectly prove that the applied PEG-400 do not contain organic impurities.

The band at 3434 cm^{-1} in IR spectrum of magnetite particles corresponds to stretching vibrations of bonded OH-groups. This line can characterize the adsorbed molecular water. The band at 2928 cm^{-1} is assigned to the vibrations of CH_2-group. Nevertheless, no characteristic peaks related to the stretching vibrations of —C—O—C— groups were recorded in the spectrum.

In the short-wavelength region of the spectrum, two broaden adsorption band at 414—438 and 587 cm^{-1} were registrated arising from the lattice vibrations of Fe—O bonds in tetral or octoedral positions.[19] The positions of the characteristic peaks owing to the vibration of these bonds are in agreement with the model spectrum.

Thus, based on the data of IR-spectroscopy, we can conclude that a fraction of the bonded free water is present on the surface of magnetite particles. At the same time no bands relating to the molecules of stabilizer were found.

In order to determine an amount of the bounded water as well as a character of the thermal transformations of magnetite, a thermal analysis of the obtained particles was performed. Figures 4 and 5 display DSC-TG measurements of Fe_3O_4 performed under inert or air atmosphere.

It should be noted that the TG curve has a complicated pattern due to the variable composition of particles which contain not only oxide and hydroxide phases but some amount of ethylene glycol.

DSC curve of the sample heated in inert atmosphere shows endothermic changes in the temperature range from 48 to 180 °C (see Fig. 4). In this interval, the mass loss of the sample was 1.93%. The obtained effect accounts for desorption of the physically adsorbed water from the

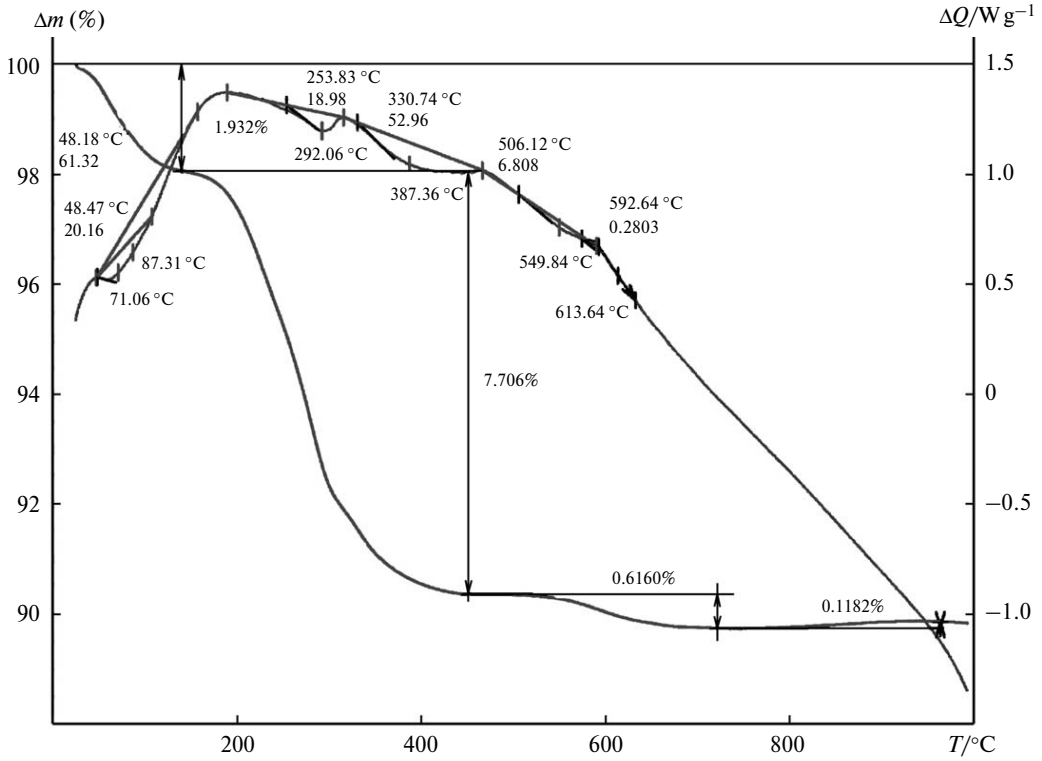

Fig. 4. DSC and TG thermograms of the magnetite particles in the inert medium. Here and on Fig. 5, numbers near the curves are *Q* ($J\ g^{-1}$).

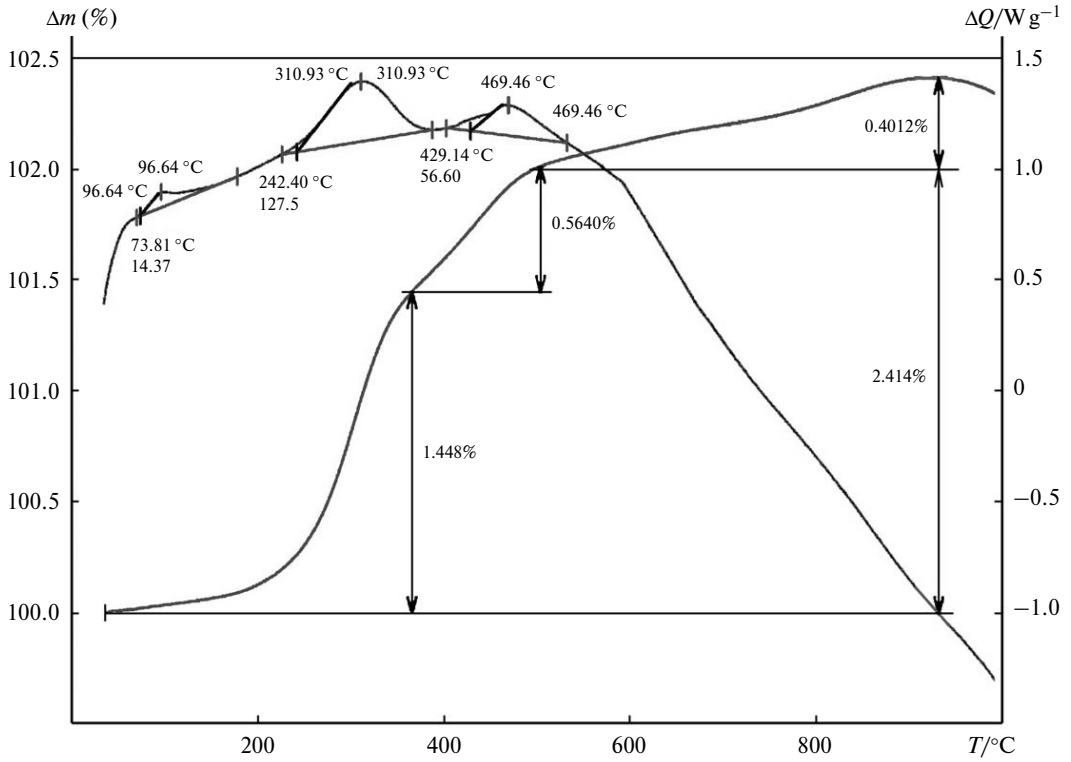

Fig. 5. DSC and TG thermograms of the magnetite particles in air.

particle surface.[20] Within the temperature ranges of 253—300 and 330—500 °C, endothermic effect is accompanied by the mass loss of 7.7%. Such heat absorption and decrease in the mass of the sample is attributed to desorption of the chemically adsorbed water.

In the range from 508 to 613 °C, an endothermic effect occurs when the mass loss of 0.6%. In this temperature region, the products of thermal destruction of ethylene glycol or polymers, formed during dehydration of the former, as well as the possible products of their reaction with an iron oxide matrix are likely to desorb.

DCS curve of the sample heated in air shows exothermal effects at 73—180 and 242—420 °C which correspond to a total increase in the sample mass for 1.45%. In the plot of correlation between a sample mass and temperature, a sharp bend at ~360 °C is observed. These phenomena are likely caused by magnetite oxidation to γ-Fe_2O_3 maghemite. In the oxidizing atmosphere (air) magnetite is not stable and is oxidized producing cation-deficient magnetite followed by maghemite formation.[21] Maghemite (γ-Fe_2O_3) is isostructural to magnetite but has smaller lattice parameters. Moreover, maghemite is also paramagnetic.

Based on TGA data, it was defined that a mass increase had to constitute 3.39% at particle oxidation, while on practice it was equal to 2.4%. That fact allows us to assume a change in mole ratio between iron(+2) and iron(+3) with an excess of Fe_2O_3 when compared with the theoretical ratio.

In the range from 429 to 469 °C, DSC curve shows exothermic effect accompanied with 0.5% increase in mass. That may be accounted for the transition of maghemite to α-Fe_2O_3 hematite. According to the literature,[21] maghemite is instable when heating and irreversibly transforms into hematite in the range from 300 to 500 °C. Hematite is an antiferromagnetic oxide, which is characterized by remarkably high thermal stability. Hence it is often the end product of transformation of the other iron oxides. In the range from 469 to 915 °C a further increase in mass of the sample for 0.4% was detected.

Influence of the mole ratio $C_2H_3O_2Na$: Fe^{3+} on magnetite particle size. When generating spherical magnetite particles, sodium acetate $C_2H_3O_2Na$, as a component of reaction mixture, provides relatively constant pH value and operates as a precursor for the formation of intermediates during the particle synthesis.

Acetate-ions not only form intermediates with iron(+3) cations but can adsorb on the surface of the generated particles, forming negative charge and preventing particle agglomeration (electrostatic factor of stabilization). Hence it is important to defite the impact of $C_2H_3O_2Na$, content, namely mole ratio $C_2H_3O_2Na$: Fe^{3+}, on the size of the synthesized Fe_3O_4 particles at the constant iron(+3) concentration.

The initial concentration of iron(+3) salt was 0.05 mol L^{-1}, mole ratio $C_2H_3O_2Na$: Fe^{3+} was varied from 3 : 1 to 15 : 1. PEG-400 concentration was 5 mmol L^{-1}.

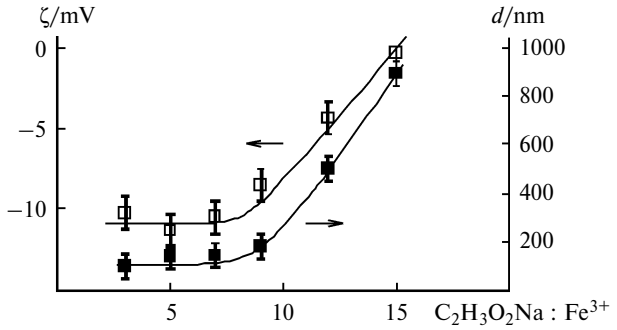

Fig. 6. Dependencies of ζ-potencial and the mean size (*d*) of magnetite particles from the mole ratio $C_2H_3O_2Na : Fe^{3+}$.

The relationship between magnetite particle size, their morphology and synthesis conditions are presented in Table 1.

The dependence of the mean particle size and concentration of sodium acetate was defined by dynamic light scattering (Fig. 6).

The obtained correlation shows that with increasing mole ratio $C_2H_3O_2Na : Fe^{3+}$ from 3 : 1 to 7 : 1 the mean particle size slightly increased and the value of ζ-potential (see Fig. 6) was nearly constant (around −10.5 mV). When the concentration of sodium acetate raised up to mole ratio $C_2H_3O_2Na : Fe^{3+}$ equal to 9 : 1, the mean particle size increased up to ~170 nm and the ζ-potential value increased up to −0.3 mV. Probably an increase in ζ-potential value is associated with compression of the electrical double layer (EDL), which is formed by adsorption of acetate ions on the particle surface. Further increase in sodium acetate content did not result in generation of particles with micron sizes.

Mössbauer spectroscopy. Mössbauer spectrum of Fe_3O_4 magnetite particles from the ^{57}Fe nuclei, recorded at 300 K ($T < T_N$, where T_N is the Neel temperature), represents a complex hyperfine Zeeman magnetic structure that reflects combined electron and magnetic interactions (Fig. 7).

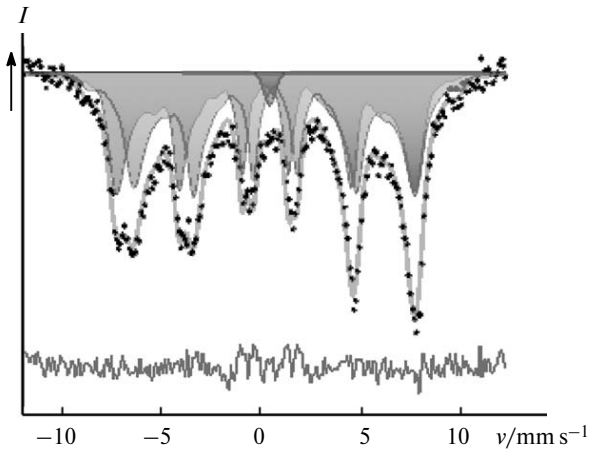

Fig. 7. Mössbauer spectra on nucleus of ^{57}Fe for the sample of magnetite, registered at 300 K; the method of the reconstructed fields was applied for the data processing.

For the given spectrum, two distributions of hyperfine magnetic field on ^{57}Fe nuclei ($p(H_{Fe})$) were reconstructed in assumption of linear correlation between chemical shift (δ), quadrupole splitting (ε) and H_{Fe} values (Fig. 8).

The spectrum is satisfactorily described as a superposition of two Zeeman sextets (Fe1, Fe2) along with paramagnetic components (singlet Fe3) (see Fig. 7). The hyperfine parameters are shown in Table 2.

Fe1 (I = 47(5)%) distribution with a mean value of chemical shift <δ> equal to 0.27(2) mm s^{-1} corresponds to the iron in the oxidation state of +3 in tetrahedral oxygen surrounding. Fe2 (I = 52(5)%) distribution with a mean value of chemical shift <δ> equal to 0.72(2) mm s^{-1} corresponds to the iron in the oxidation state of +2.5 in octahedral oxygen surrounding.[22] The values of quadrupole splitting of all the components are close to 0 mm s^{-1} that is typical of the systems with high symmetry.

When measured at 300 K, Fe^{2+} and Fe^{3+} ions in the tetrahedral and octahedral positions in magnetite are in the state of fast electron exchange, which proceeds faster compared with the resolution time of the Mössbauer spectroscopy. That is why the sextet distribution relating to the intermediate oxidation state is observed. Fe_3O_4 formula can be represented as $(Fe^{2.5+}{}_o)_2Fe^{3+}{}_tO_4$ (where Fe_o and Fe_t are iron atoms in octahedral or tetrahedral position correspondingly). In the case of stoichiometric sample, the component ratio Fe2 : Fe1 would be equal to

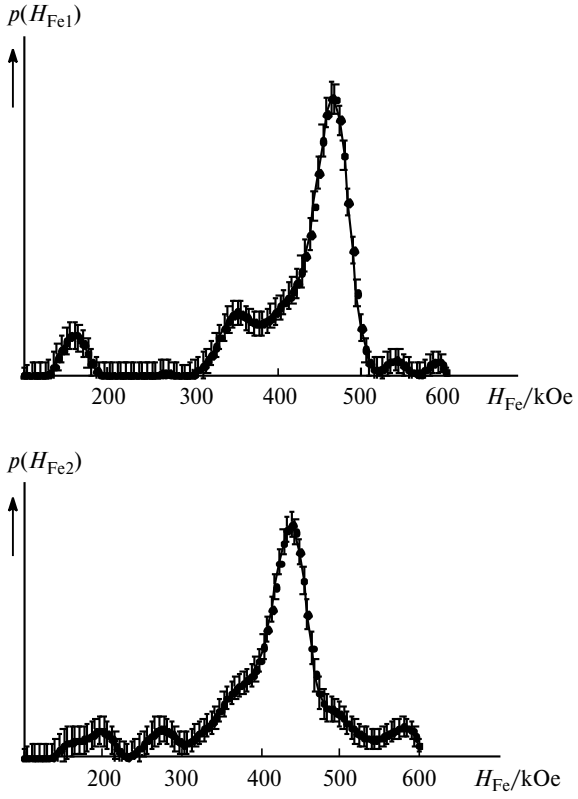

Fig. 8. Reconstructed distributions of hyperfine magnetic field on ^{57}Fe nuclei.

Table 2. Mean values of ultrafine parameters of the spectral components

Component	Area S_i (%)	<δ>	<ε>	$<H_{Fe}>$ /kOe
		mm s^{-1}		
Fe1	47(5)	0.27(2)	0.2(2)	422(13)
Fe2	52(5)	0.72(2)	0.1(2)	411(11)
Fe3	1.2(6)	0.47(7)	0	—

2 : 1. For the sample of interest it constitutes ~5 : 4, proving that iron partly transformed into trivalent state and γ-Fe_2O_3 was formed. So the formula of the substance can be described as $Fe_3O_{4+\delta}$. From the area relation of the components ($S = S_2/S_1$) the concentration of the vacancies $\delta = (2 - S)/(5S + 6)$ can be calculated.[23] For the investigated sample, $\delta = 0.07$.

The reconstracted distributions are wide. That is likely to be related with the size distribution of nanoparticles and the agglomerate formation from particles with different sizes. The average hyperfine magnetic field components are $<H_{Fe1}> = 422(13)$ kOe and $<H_{Fe2}> = 411(11)$ kOe. These magnitudes are lower than those for the large crystalline magnetite (where H_{Fe} reaches up to 500 kOe).[24]

The superparamagnetic component (Fe3) seems to correspond to those nanoparticles which did not participate in agglomerate formation. The value of the chemical shift of the component ($\delta = 0.47(7)$ mm s^{-1}) was in the error range and corresponded to octahedral coordination of Fe^{3+} ion surrounded by oxygen.[22] According to the literature,[25] 24 nm is the size at which the superparamagnetism of margnetite at 300 K is observed. The presence of superparamagnetic component indicates on that the particle sizes in the studied sample were less than the outlined above magnitude.

Magnetic properties of magnetite particles. Physical properties of nanoparticles are different from those of a bulk material due to the ratio of surface atoms. A decrease in a particle size increases the surface energy. The most topical challenge is determination of correlation between particle size and macroscopic parameters of particles as, for example, Curie temperature, coercivity residual magnetism.

We determined magnetic properties of particles with different sizes: 90, 200 and 270 nm.

The investigation showed that the specific magnetism of saturation constituted 65, 64 and 55 G cm^3 g^{-1} for the particles with sizes 90, 200 and 270 nm respectively (Fig. 9).

Bulk magnetite is a ferromagnetic with a saturation magnetization value of 80—100 G cm^3 g^{-1} at 300 K. [26]

Residual magnetization for the particles with sizes of 90 and 270 nm constituted 10 G cm^3 g^{-1} when that for the particles of 200 nm was 12 G cm^3 g^{-1}. The coercivity for all the particles was ~110 Oe (8.7 кА m^{-1}). According to the literature,[10] for the spherical particles with a size of

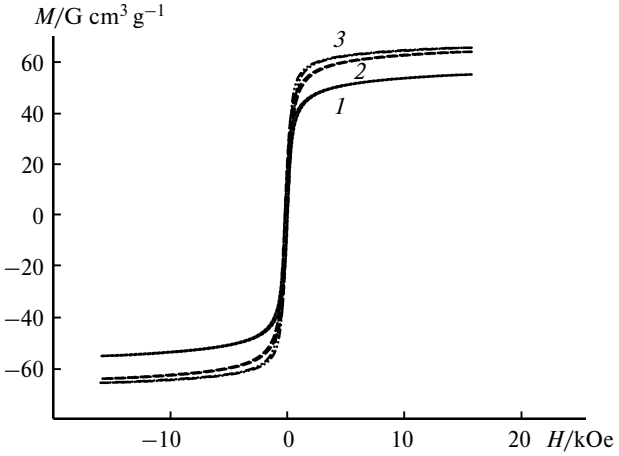

Fig. 9. Hysteresis loops for the magnetite particles with different sizes: 90 (*1*), 200 (*2*), and 270 nm (*3*).

~200 nm obtained in an autoclave the residual magnetization was 9.32 G cm^3 g^{-1}, the coercivity was 150 Oe. For the particles with an average size of 280 nm, the residual magnetization was 13.5 G cm^3 g^{-1} and coercivity was 195 Oe. Thus, our results are in accordance with those reported earlier and the synthesized particles relate to the hard magnetic materials.

The differences in magnetic properties between the studied particles and the bulk material accounted for the size effect.

To sum up, the proposed method for nano- and submicron magnetite particle generation is an alternative to that requiring autoclave application. The synthesised nano- and submicron spherical particles of magnetite seems to be agglomerates composed from nanoparticles of ~5—15 nm. By varying the reaction conditions the particles with diameters from ~50 to ~200 nm were produced. The mechanism of magnetite generation in the given system was suggested. The study of magnetic properties of the obtained particles showed that they are related to the hard magnetic materials.

The work was performed at the financial support of the Ministry of Education and Science of the Russian Federation within the aggriment for granting No. 14.576.21.0002 from 17 June, 2014 (unique identificator of the applied researches (projects) RFMEFI57614X0002).

References

1. F. Ye, A. Barrefelt, H. Asem, M. Abedi-Valugerdi, I. El-Serafi, M. Saghafian, K. Abu-Salah, S. Alrokayan, M. Muhammed, M. Hassan, *Biomaterials*, 2014, **35**, 3885.
2. P. Tartaj, M. P. Morales, S. Veintemillas-Verdaguer, T. Gonzalez-Carreno, C. J. Serna, *J. Phys. D: Appl. Phys.*, 2003, **36**, R182.

3. Y. M. Wang, X. Cao, G. H. Liu, R. Y. Hong, Y. M. Chen, X. F. Chen, H. Z. Li, B. Xu, D. G. Wei, *J. Magnetism and Magnetic Materials*, 2011, **323**, 2953.
4. M. Mahdavi, M. B. Ahmad, M. J. Haron, F. Namvar, B. Nadi, Z. Rahman, J. Amin, *Molecules*, 2013, **18**, 7533.
5. *Nanotechnology in Biology and Medicine: Methods, Devices and Applications*, Ed. T. Vo-Dinh, CRC Press Taylor and Francis Group, Boca Raton, 2007, 792 pp.
6. J. Ge, Y. Hu, Y. Yin, *Angew. Chem., Int. Ed.*, 2007, **46**, 7428.
7. H. Hu, Ch. Chen, Q. Chen, *J. Mater. Chem. C.*, 2013, **1**, 6013.
8. *Nanomaterials and Nanochemistry*, Eds C. Brechignac, P. Houdy, M. Lahmani, Springer, Berlin, 2007, 777 pp.
9. *Nanomaterials: A Danger or a Promise? A Chemical and Biological Perspective*, Eds R. Brayer, F, Fievet, Th. Coradin, Springer-Verlag, London, 2013, 399 pp.
10. T. Fan, D. Pan, H. Zhang, *Ind. Eng. Chem. Res.*, 2011, **50**, 9009.
11. H. Deng, X.L. Li, Q. Peng, X. Wang, J. P. Chen, Y. D. Li, *Angew. Chem., Int. Ed.*, 2005, **44**, 2782.
12. S. Xuan, Y.-X. J. Wang, J. C. Yu, K. C. Leung, *Chem. Mater.*, 2009, **21**, 5079.
13. US Pat. 2010/0224823 A1. Y. Yin, J. Ge, 2010; http://www.google.com/patents/US20100224823.
14. M. Lin, H. Huang, Z. Liu, Y. Liu, J. Ge, Y. Fang, *Langmuir*, 2013, **29**, 15433.
15. A. G. Savchenko, S. V. Salikhov, E. V. Yurtov, Yu. D. Yagodkin, *Bull. Russ. Acad. Sci., Physics (Int. Ed.)* 2013, **77**, 704 [*Izv. Acad. Nauk*, *Ser. Phys.*, 2013, **77**, 776].
16. S. V. Salikhov, A. G. Savchenko, I. S. Grebennikov. E. V. Yurtov, *Izv. Acad. Nauk, Ser. Phys.*, 2015, **79**, 1251 [*Bull. Russ. Acad. Sci., Physics (Int. Ed.)*, 2015, **79**].
17. Yu. D. Yagodkin, S. V. Salikhov, O. A. Ushakova, *Zavod. Lab. Diagn. Mater.*, 2013, **79**, 41 [*Inorganic Materials (Int. Ed.)*, 2013, **49**].
18. N. A. Shabanov, V. V. Popov, P. D. Sarkisov, *Khimiya i tekhnologiya nanodispersnykh oksidov* [*Chemistry and technology of nanodispersed oxides*], Akademkniga, Moscow, 2006, 309 pp. (in Russian).
19. N. V. Dikii, A. N. Dovbnya, E. V. Medvedeva, N. P. Khlapova, I. D. Fedorets, V. L. Uvarov, Yu. V. Liashko, *Vestn. Khar´kov univ.* [*Vestn. Khar´kov univ.*], 2008, **823**, 78 (in Russian).
20. Y. H. Chen, *J. Alloys Comp.*, 2013, **553**, 194.
21. P. A. Katasonov, R. A. Garifullyn, *Pis'ma o materialah* [*Lett. about materials*], 2013, **3**, 322 (in Russian).
22. F. Menil, *J. Phys. Chem. Solids*, 1985, **46**, 763.
23. H. Topse, J. Dumesic, M. Boudart, *J. Phys. Colloq.*, 1974, **35**, 411.
24. F. J. Berry, S. Skinner, M. F. Thomas, *J. Phys.: Condens. Matter*, 1998, **10**, 215.
25. A. A. Lyutoev, Yu. G. Smirnov, *Neftegazovoe Delo: electron. nauch. zhurn.* [*Oil and Gas Business: the electron. sci. j.*], 2013, **4**, 424 (in Russian).
26. *Tablithy phyzicheskih velichin* [*Tables of physical values*], Ed. I. K. Kikoin, Atomizdat, Moscow, 1976, 1006 pp. (in Russian).

Received October 20, 2015;
in revised form January 19, 2016